inorganics

MDPI

Article

Effect of Coordinating Solvents on the Structure of Cu(II)-4,4′-bipyridine Coordination Polymers

Marzio Rancan [1,*], Alice Carlotto [2], Gregorio Bottaro [1] and Lidia Armelao [1,2,*]

[1] Institute of Condensed Matter Chemistry and Technologies for Energy (ICMATE), National Research Council (CNR), c/o Department of Chemical Sciences, University of Padova, via Marzolo 1, 35131 Padova, Italy

[2] Department of Chemical Sciences, University of Padova, via Marzolo 1, 35131 Padova, Italy

* Correspondence: marzio.rancan@cnr.it or marzio.rancan@unipd.it (M.R.); lidia.armelao@unipd.it (L.A.)

Received: 23 July 2019; Accepted: 13 August 2019; Published: 19 August 2019

Abstract: Solvent can play a crucial role in the synthesis of coordination polymers (CPs). Here, this study reports how the coordinating solvent approach (CSA) can be used as an effective tool to control the nature of the final CP. This study exploited the system Cu(II)-4,4′-bipyridine coupled to different coordinating solvents, such as DMA, DMF and DMSO. This allowed the isolation and structurally characterization of four new CPs: three 2D layered networks and one 1D chain. Moreover, it was evidenced that even adventitious water can play the role of the coordinating solvent in the final CP.

Keywords: coordination polymer; MOF; CP; dimensionality control; Cu(II)-4,4′-bipyridine; dipyridil ligand; copper

1. Introduction

Coordination polymers (CPs) and metal organic frameworks (MOFs) have attracted increasing interest over the last two decades since the features of these systems are potentially useful in several cutting-edge research areas [1–3]. Countless studies have been devoted by researchers to these compounds, however there are still controversial opinions as to whether a real design of these systems can be applied [4–6]. In fact, the predictability of the final network can be a challenge since it is a consequence of the self-assembly process that involves competing, reversible and simultaneous interactions among the metal, ligand, counterion and solvent, just to mention the main chemical actors. In this context, the energy of the metal-ligand bond plays a crucial role. Metal ions and charged ligands (for instance carboxylates) can give quite strong bonds (200–400 kJ/mol ca.) paving the route to the so-called reticular chemistry that allows a good design of the final MOF [7]. This strategy has been used to develop large families of structures where the network can be designed combining the starting building blocks and at the same time, the pores size can be controlled by simply varying the length of the ligand maintaining the same network topology and obtaining isoreticular MOFs [8,9]. On the other hand, when considering weaker interactions, as for instance metal ions and neutral ligands (60–180 kJ/mol ca.), the final coordination outcome is not easy to control, both in terms of topology and network dimensionality. In fact, as the interaction energy between metal and ligand decreases, the system is more prone to be affected by other parameters, such as the counterion and the solvent. In particular, when considering Cu(II) and the 4,4′-bipyridine ligand (bpy), many different CPs and MOFs can be obtained. The isolated structure strongly depends on the counterion leading, for instance, to systems with different dimensionalities (1D, 2D and 3D) and topologies [10–14]. In addition, the solvent can play an important role. For instance, the 2D $[Cu(bpy)_2(CF_3SO_3)_2]_n$ framework can be transformed into a hydrogen bond assisted 3D framework through a solvent (H_2O) mediated process [15] and solvent dependent routes were developed to obtain 2D or 3D $[Cu(bpy)_2(CF_3SO_3)_2]_n$

networks [16]. In this context, the authors previously showed that a coordinating solvent, such as dimethyl sulfoxide (DMSO), can be used to tune and control the dimensionality of the final CP [17]. This coordinating solvent approach (CSA) promotes dimensional variability, driving the formation of Cu–bpy architectures, such as a 3D nanoporous network ($\{[Cu_2(bpy)_4(DMSO)_3(ClO_4)](ClO_4)_3{\cdot}2DMSO\}_n$, **1**) or a 1D chiral chain ($\{[Cu(bpy)_2(DMSO)_4](ClO_4)_2\}_n$, **2**) just changing the crystallization conditions (i.e., the presence of a co-solvent or evaporation rate). In solution, DMSO and bpy molecules establish a series of dynamic equilibria to coordinate the metal center during the self-assembly process. The coordinating solvent can block a different number of coordination sites leading to different CP architectures. Recently, the authors have also demonstrated that Cu–bpy bonds and coordinating solvents can be used to reversibly self-assemble mechanically interlocked CPs, such as the coordination-driven polyrotaxane-like architectures [18], when employing a Cu–metallocycle as a platform for the self-assembly of the Cu–bpy extend architectures.

Herein, this study extended CSA to other coordinating solvents (*N*,*N*-dimethylformamide, DMF; *N*,*N*-dimethylacetamide, DMA; and mixtures of them) and their effect on the final Cu–bpy based CPs were studied. Moreover, it was also demonstrated that even water can participate as a coordinating solvent during the dynamic equilibria that lead to the final CP. All the new compounds have been isolated as single crystals and structurally characterized resulting in three new 2D and one 1D CPs.

2. Results

All the CPs (**3**–**6**) were synthesized by dissolving $Cu(ClO_4)_2{\cdot}6(H_2O)$ in a coordinating solvent and adding bpy in a 1:2 ratio. The solvent evaporation or diffusion of a co-solvent allowed isolating single crystals of the compounds. All the structures were solved by the single-crystal X-ray crystallographic method and their phase purity confirmed by powder X-ray diffraction (PXRD, Figure S1). The important refinement and geometric parameters are shown in Table 1.

Table 1. Crystal data and structures refinement.

Compound	3	4	5	6
Formula	$C_{28}H_{38}Cl_2CuN_6O_{12}$	$C_{46}H_{46}Cl_2CuN_{10}O_{10}$	$C_{40}H_{36}Cl_2CuN_8O_{11}$	$C_{20}H_{34}Cl_2CuN_4O_{12}S_2$
Formula weight	785.08	1033.37	939.21	721.07
Temperature/K	301(2)	301(3)	301.2(8)	299.6(6)
Crystal system	monoclinic	monoclinic	monoclinic	monoclinic
Space group	*C*2/*c*	$P2_1/n$	*P*2/*n*	*I*2/a
a/Å	14.4924(10)	10.2921(4)	12.9264(5)	17.9524(17)
b/Å	11.1385(7)	15.7544(4)	11.1702(4)	11.0913(7)
c/Å	22.2237(13)	15.3205(5)	15.0564(10)	16.3512(15)
α/°	90	90	90	90
β/°	91.562(7)	106.641(4)	106.559(6)	100.154(8)
γ/°	90	90	90	90
Volume/Å^3	3586.1(4)	2380.11(14)	2083.83(19)	3204.8(5)
Z	4	2	2	4
Goodness-of-fit on F^2	1.117	1.024	1.081	1.035
Final R indexes [$I >= 2\sigma(I)$]	R_1 = 0.0575, wR_2 = 0.1683	R_1 = 0.0338 wR_2 = 0.0914	R_1 = 0.0473 wR_2 = 0.1279	R_1 = 0.0340 wR_2 = 0.0843
Largest diff. peak/hole/e Å^{-3}	0.60/−0.40	0.35/−0.25	0.62/−0.71	0.35/−0.32
CCDC	1942113	1942114	1942115	1942116

By using DMA, light blue single crystals of $\{[Cu(bpy)_2(H_2O)_2](ClO_4)_2{\cdot}2DMA\}_n$ (**3**) were obtained in good yield (70% ca.). An X-ray analysis evidenced that four bpy molecules in the equatorial plane and two water molecules in apical positions coordinated the copper center, Figure 1a. The copper atom has a Jahn–Teller distorted octahedral coordination with Cu–N distances of 2.027(4), 2.036(6) Å and 2.047(6) (for Cu1–N1, Cu1–N2 and Cu1–N3, respectively) and a Cu1–O1 bond length of 2.482(2) Å. The water molecule forms H-bonds with a ClO_4^- anion (2.275(9) Å) and with a DMA molecule (1.972(5) Å). The network develops as a 2D CP, leading to layers of grids composed of repeating squares with

Cu–bpy–Cu sides (Figure 1b). Two slightly different Cu–bpy–Cu distances can be found, one of 11.1385(7) Å coinciding with the *b* axis and the other of 11.1165(7) Å along the *c* axis equal to half its length. The 2D layers are at a distance of *a*/2 (7.3462(5) Å) and mismatched along the *b* axis with a value of *b*/2 (Figure 1c). This packing of the grids layers leads to the formation of two different alternating channels (Figure 1d) that occupy the 66% of unit cell volume. In one case, the plane containing the bpy molecules of a grid is parallel to the grow direction of the channel. In the other one, that plane is perpendicular to the channel direction. Perchlorate anions and DMA molecules that lay between the grid layers fill the channels.

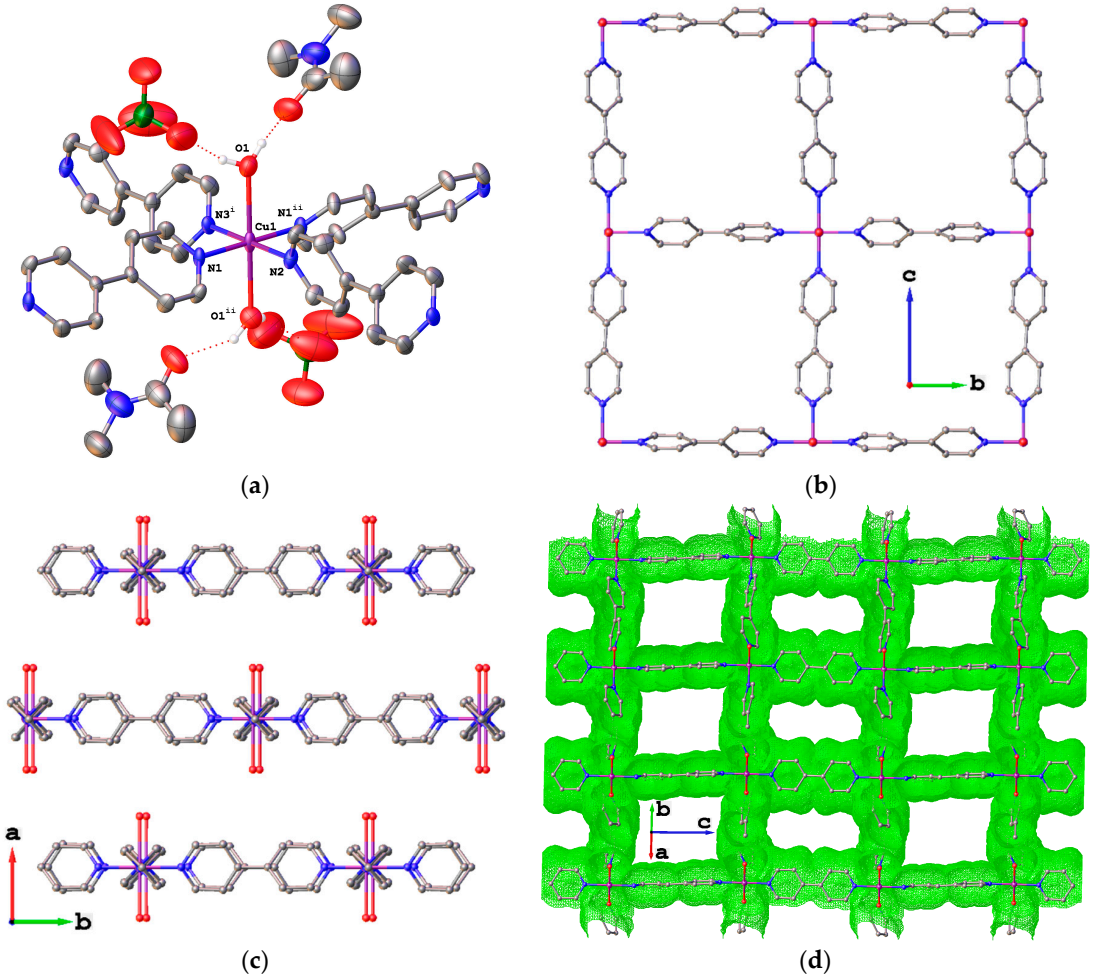

Figure 1. (**a**) Coordination environment of the copper center in compound **3** (thermal ellipsoids drawn at the 50% probability level). (**b**) 2D network (single layer); (**c**) view along the *ab* plane of alternating and mismatched grids; (**d**) channels formed by the 2D layers (green points). Color code: Cu, purple; O, red; N, blue; C, grey; Cl, green; H, white. Anions, DMA molecules and H atoms omitted for clarity in the packing figures. Symmetry operations: $i = 1 - x, -1 + y, 1/2 - z$; $ii = 1 - x, +y, 1/2 - z$.

When DMF was used in place of DMA, the solvent evaporation at open air led to a major crop (yield 40% ca.) of deep blue single crystals of $\{[Cu(bpy)_2(DMF)_2](ClO_4)_2{\cdot}2(bpy)\}_n$ (**4**) along with a minor fraction (yield 3% ca.) of light blue single crystals of $\{[Cu(bpy)_2(H_2O)_2](ClO_4)_2{\cdot}2(bpy){\cdot}2(H_2O)\}_n$ (**5**).

Considering compound **4**, four bpy molecules in the equatorial plane coordinate the copper center and the apical positions are occupied by DMF molecules (Figure 2a). Copper has a Jahn–Teller distorted octahedral coordination with Cu–N distances of 2.0250(12), 2.0564(12) Å (for Cu1–N1 and Cu1–N2, respectively) and a Cu1–O1 bond length of 2.5180(12) Å. Even **4** is a 2D CP with layers of grids (Figure 2b) composed of repeating squares with Cu–bpy–Cu sides of 11.1640(3) Å and one

Cu···Cu diagonal coinciding with *b* axis (15.7544(4) Å). The 2D layers in **4** are at a distance of 10.3 Å and mismatched of 5.6 Å (Figure 2c). This layer packing leads to the formation of only one kind of channels (Figure 2d) that occupies 57% of the unit cell volume. These channels are filled by the ClO_4^- anions that lay between the grid layers and by uncoordinated bpy molecules hosted in the Cu–bpy squares. In particular, each square hosts two bpy molecules that interacts with the CP network with a series of CH···π interactions and among them by π···π stacking (Figure 2e,f).

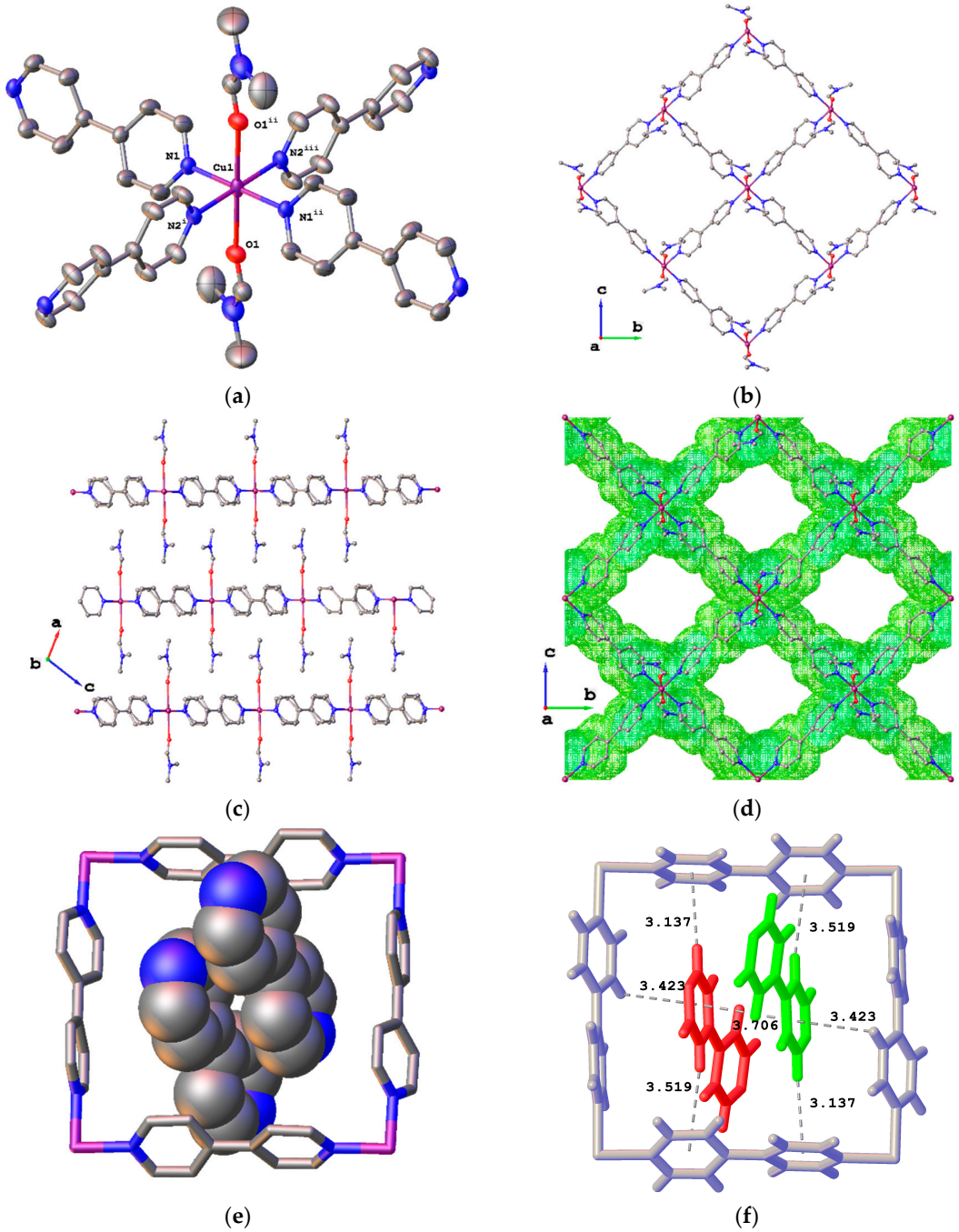

Figure 2. (**a**) Coordination environment of the copper center in compound **4** (thermal ellipsoids drawn at the 50% probability level). (**b**) 2D network (single layer); (**c**) view along the *ac* plane of alternating and mismatched grids; (**d**) channels formed by the 2D layers (green points). (**e**) Two uncoordinated bpy molecules hosted by a Cu–bpy square. (**f**) CH···π interactions and π···π stacking in the host-guest ensemble. Color code: Cu, purple; O, red; N, blue; C, grey. Anions and H atoms omitted for clarity. Symmetry operations: *i* = 2 − *x*, 1 − *y*, 1 − *z*; *ii* = 1/2 + *x*, 3/2 − *y*, 1/2 + *z*; *iii* = 3/2 − *x*, 1/2 + *y*, 1/2 − *z*.

In CP **5**, the coordination environment of the Cu^{2+} ions is similar, as in CP **3**. The four bpy molecules in the equatorial plane and the two water molecules in apical positions coordinate the copper center (Figure 3a). The metal atom has a Jahn–Teller distorted octahedral coordination with Cu–N distances of 2.0670(19), 2.041(3) Å and 2.045(3) (for Cu1–N1, Cu1–N2 and Cu1–N3, respectively) and a Cu1–O1 bond length of 2.4965(19) Å. Similar to **3** and **4**, the network develops as a 2D CP, leading to layers of grids composed of repeating squares with Cu–bpy–Cu sides (Figure 3b). Further in CP **5**, the apical water molecules form H-bonds with a ClO_4^- anion (2.128(3) Å) and with an uncoordinated bpy molecule (2.005(3) Å). The side of the bpy molecule not involved in the H-bond is diagonally pointing towards the center of a Cu–bpy square of a second grid layer. In this case, the starting DMF coordinating solvent is not found in the structure. Two slightly different Cu–bpy–Cu distances can be found: one of 11.1702(4) Å coinciding with the *b* axis and the other of 11.2841(6) Å. The 2D layers in **5** are at a closer distance (8.3 Å) compared to **3** and only slightly mismatched (Figure 3c). This layer packing leads to the formation of only one kind of channels (Figure 3d) that occupies 70% of the unit cell volume. Perchlorate anions and bpy molecules, that lay between and inside (bpy) the grid layers, fill those channels.

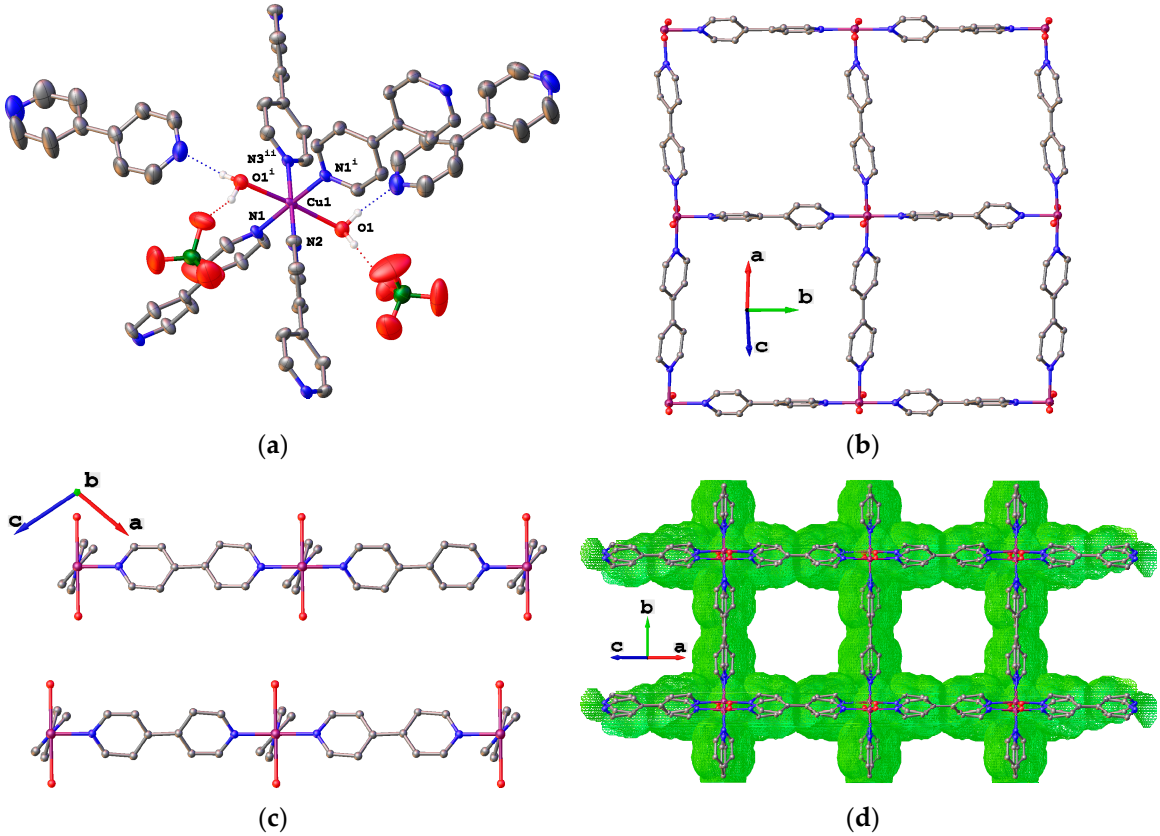

Figure 3. (**a**) Coordination environment of the copper center in compound **5** (thermal ellipsoids drawn at the 50% probability level). (**b**) 2D network (single layer); (**c**) view along the *ac* plane of alternating and slightly mismatched grids; (**d**) channels formed by the 2D layers (green points). Color code: Cu, purple; O, red; N, blue; C, grey; Cl, green; H, white. Anions, uncoordinated bpy molecules and H atoms omitted for clarity in the packing figures. Symmetry operations: $i = 1/2 - x, +y, 1/2 - z$; $ii = +x, -1 - y, +z$.

It is worthy to note that both CPs **3** and **5** are obtained with coordinated water molecules instead of the solvents, DMA or DMF. This is an important difference compared to what happens when using DMSO as a coordinating solvent [17]. In that case, slow evaporation led to a Cu–bpy based 3D CP (**1**) while faster evaporation gave a 1D chiral chain (**2**). In both cases, the only solvent coordinating the

Cu center was DMSO. However, it was postulated that in the CSA, the role of water as competitive coordinating solvent may not be excluded. As a matter of fact, synthesis with DMA and DMF confirmed our hypothesis. The sources of water can be found in the hydration water molecules of the starting $Cu(ClO_4)_2$, in the non-anhydrous solvents, or even in the evaporation performed at open air.

Finally, the employment of mixtures of coordinating solvents was explored. DMA/DMF, DMF/DMSO and DMA/DMSO 1:1 solutions evaporation did not give any crystalline product suitable for single crystal X-ray diffraction. Very slow vapor diffusion of diethylether in a DMF/DMSO mixture led to light blue single crystals of $\{[Cu(bpy)_2(DMF)(DMSO)](ClO_4)_2\}_n$ (**6**, Figure 4) in low yields (10% ca.). The X-ray structure shows that copper has a Jahn–Teller distorted octahedral coordination with the equatorial positions taken by two bpy molecules (Cu1–N1 and Cu1–N2 2.004(2) Å) and two DMSO molecules (Cu1–O1 2.0114(15) Å). The axial positions are occupied by two DMF molecules (Cu1–O2 2.3662(17) Å). The CP develops as a 1D chain with a Cu–bpy–Cu distance of 11.0913(7) Å coinciding with *b* axis. The chain grow linearly since the two bpy molecules lay in equatorial *trans* positions. On the contrary, when using only DMSO, the bpy ligands take two equatorial *cis* positions leading to a helicoidal 1D CP isolated as enantiopure single crystals (**2**) [17].

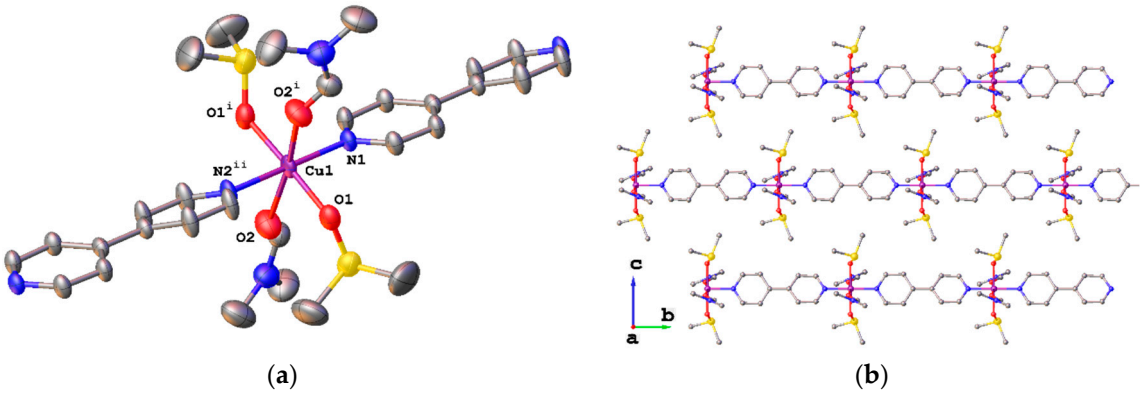

(**a**) (**b**)

Figure 4. (**a**) Coordination environment of the copper center in compound **6** (thermal ellipsoids drawn at the 50% probability level). (**b**) 1D chains along the plane *cb*. Color code: Cu, purple; O, red; N, blue; C, grey; S, yellow. Anions and H atoms omitted for clarity. Symmetry operations: $i = 3/2 - x, +y, 1 - z$; $ii = 3/2 - x, -1 + y, 1 - z$.

3. Discussion

By employing strong coordinating solvents coupled to a neutral ligand, such as bpy, competitive coordination equilibria are introduced in the self-assembly process. The core concept of the CSA is depicted in Figure 5. The results obtained in the authors current and former [17] studies on the effect of coordinating solvents towards the final Cu–bpy based CPs are summarized in Table 2.

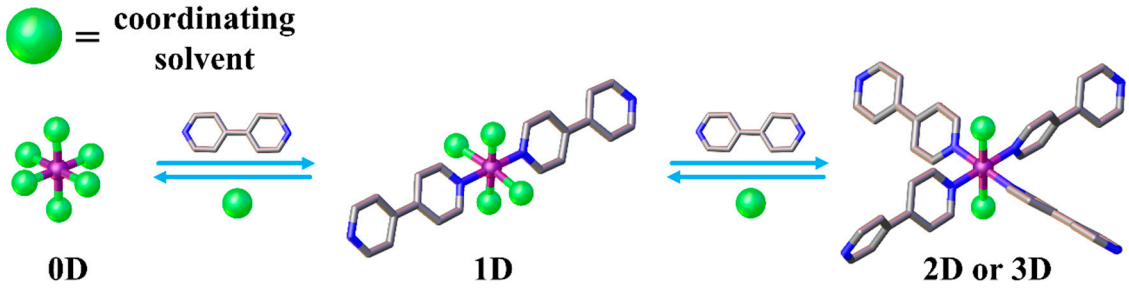

Figure 5. Scheme of the competing equilibria between the coordinating solvent and bridging ligand leading to different coordination polymers (CPs) through the coordinating solvent approach (CSA).

Table 2. The effect of coordinating solvents towards the final Cu–bpy based CPs.

Solvent.	CP	Coordinated Solvent	CP Dimensionality
DMSO [1]	**1** [17]	2 DMSO	3D
DMSO [2]	**2** [17]	4 DMSO	1D
DMA [1]	**3**	2 H_2O	2D
DMF [1]	**4** [3]	2 DMF	2D
DMF [1]	**5** [4]	2 H_2O	2D
DMSO/DMF [2]	**6**	2 DMSO + 2 DMF	1D

[1] slow evaporation; [2] in the presence of a non-coordinating solvent; [3] major product; [4] minor product.

The competitive equilibria are driven towards the CP by solvent evaporation or by introducing a co-solvent to change the medium features and to induce crystallization. Hence, when dissolving the metal center in a coordinating solvent, the process leading to the formation of the final CP can be described as the subsequent substitution of the coordinated solvent molecules by the bridging ligands. Thus, the solvent becomes itself a ligand that can compete with the bpy. This allows obtaining CPs with different networks and dimensionalities according to the solvent nature, the crystallization technique and to the remaining number of the coordinated solvent molecules versus the divergent ligands. Competitive species are present and this can lead to obtaining byproducts in low yields as in the case of CP **5**. This byproduct of CP **4** appears in the last stages of solvent evaporation and can be easily avoided by stopping the evaporation before completeness. Some general trends for the CSA applied to Cu–bpy systems can be found. The bridging bpy molecules always occupy the equatorial positions of the Cu octahedral coordination sphere. When four solvent molecules coordinate the copper (II) ion, 1D chains can be obtained, with the bpy molecules either in *trans* (CP **6**) or *cis* (CP **2**) positions. The presence of two apical solvent molecules in the coordination sphere always leads to the same structural motif, i.e., Cu–bpy squares forming extended grid-like architectures that can develop towards 2D (CPs **3**, **4**, **5**) or 3D (CP **1**) networks. Finally, it is worth noting that, when using DMA or DMF, it is likely to obtain CPs with coordinated water molecules instead of DMA or DMF ones, either as a single isolated product (**3**) or as an impurity (**5**).

4. Materials and Methods

4.1. Synthesis

The reagents were purchased from Sigma-Aldrich (St. Louis, MO, USA) and used as received. The elemental analyses were carried out with a Flash 2000 Thermo Scientific analyzer (Thermo Fisher Scientific, Cambridge, UK) at the Department of Chemical Sciences of the University of Padova.

4.1.1. Synthesis of $\{[Cu(bpy)_2(H_2O)_2](ClO_4)_2 \cdot 2DMA\}_n$ (**3**)

$Cu(ClO_4)_2 \cdot 6H_2O$ (37 mg, 0.1 mmol) was dissolved in 10 mL of DMA in a large beaker and 4,4′-bipyridine (bpy, 30 mg, 0.2 mmol) was added. The slow evaporation of the solvent led to light blue single crystals suitable for an X-ray analysis. Yield 55 mg, 70% (based on copper). The elemental analysis for $C_{28}H_{38}Cl_2CuN_6O_{12}$, exp (%): C 42.53, N 10.58, H 4.92; calc (%): C 42.84, N 10.70, H 4.88.

4.1.2. Synthesis of $\{[Cu(bpy)_2(DMF)_2](ClO_4)_2 \cdot 2(bpy)\}_n$ (**4**) and $\{[Cu(bpy)_2(H_2O)_2](ClO_4)_2 \cdot 2(bpy) \cdot 2(H_2O)_2\}_n$ (**5**)

$Cu(ClO_4)_2 \cdot 6H_2O$ (37 mg, 0.1 mmol) was dissolved in 10 mL of DMF in a large beaker and 4,4′-bipyridine (bpy, 30 mg, 0.2 mmol) was added. The slow evaporation of the solvent led to deep blue single crystals of **4**. If the solvent was left to completely evaporate, a second kind of light blue single crystals appeared in the last evaporation stages as an impurity (**5**, yield 3 mg, 3% ca.). Due to their different color, the two species can be easily manually separated. To avoid crystallization of CP **5**,

single crystals of compound **4** was removed from the solution before complete evaporation with a yield of 43 mg, 40% (based on copper). The elemental analysis for **4**, $C_{46}H_{46}Cl_2CuN_{10}O_{10}$, exp (%): C 53.31, N 13.44, H 4.56; calc (%): C 53.47, N 13.55, H 4.49. The elemental analysis for **5**, $C_{40}H_{40}Cl_2CuN_8O_{11}$, exp (%): C 51.72, N 11.98, H 4.21; calc (%): C 51.93, N 11.88, H 4.27.

4.1.3. Synthesis of $\{[Cu(bpy)_2(DMF)(DMSO)](ClO_4)_2\}_n$ (**6**)

$Cu(ClO_4)_2 \cdot 6H_2O$ (37 mg, 0.1 mmol)) was dissolved in 1 mL of a DMSO/DMF (1:1) solution and 4,4′-bipyridine (bpy, 30 mg, 0.2 mmol) was added. The very slow diffusion of diethylether vapor gave light blue single crystals after 6 weeks. Yield 8 mg, 10% (based on copper). The elemental analysis for $C_{20}H_{34}Cl_2CuN_4O_{12}S_2$, exp (%): C 33.37, N 8.01, S 9.05, H 4.83; calc (%): C 33.31, N 7.77, S 8.89, H 4.75.

4.2. Crystal Structure Determination

The data were collected using an Oxford Diffraction Gemini E diffractometer (Oxford Diffraction, Oxfordshire, England), equipped with a 2K × 2K EOS CCD area detector and sealed-tube Enhance (Mo) and (Cu) X-ray sources. The single crystals of compounds were fastened on the top of a Lindemann glass capillary. The data were collected by means of the ω-scans technique using graphite-monochromated radiation. The detector distance was set at 45 mm. The diffraction intensities were corrected for Lorentz/polarization effects as well as with respect to the absorption. The empirical multi-scan absorption corrections using equivalent reflections were performed with the scaling algorithm SCALE3 ABSPACK. The data reduction, finalization and cell refinement were carried out through the CrysAlisPro software (1.171.38.46, Rigaku Oxford Diffraction, Rigaku Corporation, Oxford, UK). The accurate unit cell parameters were obtained by least squares refinement of the angular settings of the strongest reflections, chosen from the whole experiment. The structures were solved with *Olex2* [19] by using *ShelXT* [20] structure solution program by Intrinsic Phasing and refined with the *ShelXL* [21] refinement package using least-squares minimization. In the last cycles of refinement, non-hydrogen atoms were refined anisotropically. Hydrogen atoms were included in the calculated positions, and a riding model was used for their refinement. For CP **3**, the indexing of the collected data and frame inspections clearly showed twining signals. The data were processed with the twin/multicristal routine of the CrysAlisPro software. The logout of the twin data reduction is given as Supplementary Materials. The twin data reduction with two components allowed solving the structure. The two components were rotated at 180° around the [001] vector. The final refined BASF parameter was 0.389(2). The specific refinement details for each compounds are embedded in their CIF files given as Supplementary Materials and that have been deposited with the Cambridge Crystallographic Data Centre as supplementary publication (CCDC 1942113–1942116). Copies of the data can be obtained free of charge on application to the CCDC, 12 Union Road, Cambridge CB2 1EZ, U.K. (fax, (+44) 1223 336033; e-mail, deposit@ccdc.cam.ac.uk).

4.3. Powder X-ray Diffraction (PXRD)

The PXRD patterns of CP **3** and **4** were collected with a Bruker D8 Advance diffractometer (Bruker AXS, Karlsruhe, Germany), in Bragg–Brentano geometry, using Cu Kα. The patterns were acquired in the 5°−50° 2θ range (0.03°/step and 10 s/step). The PXRD patterns of CP **5** and **6** were collected with the powder diffraction tool of an Oxford Diffraction Gemini E diffractometer using Cu Kα. The powder diffraction images (20 frames) were collected over 100 s exposition time with a 90 degrees ϕ rotation and a detector distance of 120 mm.

5. Conclusions

This study analyzed and studied the effect of coordinating solvents on the final outcome of the self-assembly process towards Cu(II)-4,4′-bipyridine based coordination polymers. Solvents such as DMA, DMF and DMSO can compete with the bridging ligand in occupying two or four coordination sites of the metal center. In this competition, also adventitious water can participate. This allowed the access to different coordination polymers. In particular, it was found that the presence of four

coordinating solvent molecules lead to 1D polymers, while two solvent molecules, in the apical sites, always gave the same fundamental unit (Cu–bpy square) that developed in grid-like structures to give 2D or 3D networks. Our results show that the coordinating solvent approach (CSA) can be used as an effective tool to modulate and control the dimensionality, composition and network of coordination polymers.

Supplementary Materials: The following are available online at http://www.mdpi.com/2304-6740/7/8/103/s1, Figure S1: PXRD patterns; CIF and checkCIF files of the crystal structures, and twin logout for CP **3**.

Author Contributions: Conceptualization, M.R.; validation M.R. and L.A.; investigation M.R., A.C. and G.B.; writing—original draft preparation, M.R. and L.A.; writing—review and editing, all authors; funding acquisition, M.R. and L.A.

Funding: This research was funded by the University of Padova (grant: P-DISC #CARL-SID17 BIRD2017-UNIPD), project CHIRoN and by Ministero Istruzione Università e Ricerca, MIUR (PRIN 2015, 20154X9ATP, Progetti di Ricerca di Interesse Nazionale. APC was sponsored by MDPI.

Conflicts of Interest: The authors declare no conflict of interest. The funders had no role in the design of the study; in the collection, analyses, or interpretation of data; in the writing of the manuscript, or in the decision to publish the results.

References

1. Kitagawa, S.; Kitaura, R.; Noro, S. Functional Porous Coordination Polymers. *Angew. Chem. Int. Ed.* **2004**, *43*, 2334–2375. [CrossRef] [PubMed]
2. Furukawa, H.; Cordova, K.E.; O'Keeffe, M.; Yaghi, O.M. The Chemistry and Applications of Metal–Organic Frameworks. *Science* **2013**, *341*, 1230444. [CrossRef] [PubMed]
3. Zhou, H.-C.; Long, J.R.; Yaghi, O.M. Introduction to Metal–Organic Frameworks. *Chem. Rev.* **2012**, *112*, 673–674. [CrossRef] [PubMed]
4. Jansen, M.; Schön, J.C. "Design" in Chemical Synthesis—An Illusion? *Angew. Chem. Int. Ed.* **2006**, *45*, 3406–3412. [CrossRef] [PubMed]
5. O'Keeffe, M. Design of MOFs and intellectual content in reticular chemistry: A personal view. *Chem. Soc. Rev.* **2009**, *38*, 1215–1217. [CrossRef]
6. Goesten, M.G.; Kapteijn, F.; Gascon, J. Fascinating chemistry or frustrating unpredictability: Observations in crystal engineering of metal–organic frameworks. *CrystEngComm* **2013**, *15*, 9249–9257. [CrossRef]
7. Yaghi, O.M. Reticular Chemistry—Construction, Properties, and Precision Reactions of Frameworks. *J. Am. Chem. Soc.* **2016**, *138*, 15507–15509. [CrossRef]
8. Eddaoudi, M.; Kim, J.; Rosi, N.; Vodak, D.; Wachter, J.; O'Keeffe, M.; Yaghi, O.M. Systematic design of pore size and functionality in isoreticular MOFs and their application in methane storage. *Science* **2002**, *295*, 469–472. [CrossRef]
9. Deng, H.; Grunder, S.; Cordova, K.E.; Valente, C.; Furukawa, H.; Hmadeh, M.; Gándara, F.; Whalley, A.C.; Liu, Z.; Asahina, S.; et al. Large-pore apertures in a series of metal–organic frameworks. *Science* **2012**, *336*, 1018–1023. [CrossRef]
10. Noro, S.; Kitaura, R.; Kondo, M.; Kitagawa, S.; Ishii, T.; Matsuzaka, H.; Yamashita, M. Framework Engineering by Anions and Porous Functionalities of Cu(II)/4,4′-bpy Coordination Polymers. *J. Am. Chem. Soc.* **2002**, *124*, 2568–2583. [CrossRef]
11. Carlucci, L.; Cozzi, N.; Ciani, G.; Moret, M.; Proserpio, D.M.; Rizzato, S. A three-dimensional nanoporous flexible network of 'square-planar' copper(II) centres with an unusual topology. *Chem. Commun.* **2002**, 1354–1355. [CrossRef]
12. Blake, A.J.; Hill, S.J.; Hubberstey, P.; Li, W.-S. Rectangular grid two-dimensional sheets of copper(II) bridged by both co-ordinated and hydrogen bonded 4,4′-bipyridine (4,4′-bipy) in $[Cu(\mu\text{-}4,4'\text{-bipy})(H_2O)_2(FBF_3)_2]\cdot 4,4'\text{-bipy}$. *J. Chem. Soc. Dalt. Trans.* **1997**, 913–914. [CrossRef]
13. Masciocchi, N.; Cairati, P.; Carlucci, L.; Mezza, G.; Ciani, G.; Sironi, A. Ab-initio X-ray powder diffraction structural characterization of co-ordination compounds: Polymeric $[\{MX_2(bipy)\}_n]$ complexes (M = Ni or Cu; X = Cl or Br; bipy = 4,4′-bipyridyl). *J. Chem. Soc. Dalt. Trans.* **1996**, 2739–2746. [CrossRef]

14. Rizzato, S.; Moret, M.; Beghi, F.; Lo Presti, L. Crystallization and structural properties of a family of isotopological 3D-networks: The case of a 4,4′-bipy ligand–M^{2+} triflate system. *CrystEngComm* **2018**, *20*, 3784–3795. [CrossRef]
15. Komori-Orisaku, K.; Hoshino, K.; Yamashita, S.; Koide, Y. Water Molecules as Binders in Transformation of 2D Coordination Polymer $[Cu(4,4'\text{-bpy})_2(OTf)_2]_n$ into Parallel Aligned 3D Architectures. *Bull. Chem. Soc. Jpn.* **2010**, *83*, 276–278. [CrossRef]
16. Kondo, A.; Kajiro, H.; Noguchi, H.; Carlucci, L.; Proserpio, D.M.; Ciani, G.; Kato, K.; Takata, M.; Seki, H.; Sakamoto, M.; et al. Super Flexibility of a 2D Cu-Based Porous Coordination Framework on Gas Adsorption in Comparison with a 3D Framework of Identical Composition: Framework Dimensionality-Dependent Gas Adsorptivities. *J. Am. Chem. Soc.* **2011**, *133*, 10512–10522. [CrossRef] [PubMed]
17. Rancan, M.; Armelao, L. Exploiting dimensional variability in coordination polymers: Solvent promotes reversible conversion between 3D and chiral 1D architectures. *Chem. Commun.* **2015**, *51*, 12947–12949. [CrossRef]
18. Truccolo, G.; Tessari, Z.; Tessarolo, J.; Quici, S.; Armelao, L.; Rancan, M. A Cu(II) metallocycle for the reversible self-assembly of coordination-driven polyrotaxane-like architectures. *Dalt. Trans.* **2018**, *47*, 12079–12084. [CrossRef]
19. Dolomanov, O.V.; Bourhis, L.J.; Gildea, R.J.; Howard, J.A.K.; Puschmann, H. *OLEX2*: A complete structure solution, refinement and analysis program. *J. Appl. Crystallogr.* **2009**, *42*, 339–341. [CrossRef]
20. Sheldrick, G.M. IUCr *SHELXT*—Integrated space-group and crystal-structure determination. *Acta Crystallogr. Sect. A Found. Adv.* **2015**, *71*, 3–8. [CrossRef]
21. Sheldrick, G.M. Crystal structure refinement with *SHELXL*. *Acta Crystallogr. Sect. C Struct. Chem.* **2015**, *71*, 3–8. [CrossRef]